Author Manuscript
Author Manuscript
Author Manuscript
Author Manuscript

HHS Public Access
Author manuscript
J Invest Dermatol. Author manuscript; available in PMC 2017 December 13.

Published in final edited form as:
J Invest Dermatol. 2016 September ; 136(9): 1885–1891. doi:10.1016/j.jid.2016.05.107.

CD301b+ Macrophages Are Essential for Effective Skin Wound Healing

Brett Shook[1], **Eric Xiao**[1], **Yosuke Kumamoto**[2], **Akiko Iwasaki**[2,3], and **Valerie Horsley**[1,4]

[1]Department of Molecular, Cellular and Developmental Biology, Yale University, New Haven, Connecticut, USA

[2]Department of Immunobiology, Yale University School of Medicine, New Haven, Connecticut, USA

[3]Howard Hughes Medical Institute, Yale University School of Medicine, New Haven, USA

[4]Department of Dermatology, Yale School of Medicine, New Haven, Connecticut, USA

Abstract

Regeneration of skin's barrier function after injury requires temporally coordinated cellular interactions between multiple cell types. Macrophages are essential inflammatory cells in skin wound regeneration. These cells switch their phenotype from inflammatory in the early regenerative stages to anti-inflammatory in the midstages of healing to coordinate skin repair. However, little is known about how different subsets of anti-inflammatory macrophages contribute to skin wound healing. Here, we characterize midstage macrophages ($CD45^+/CD11b^+/F4\text{-}80^+$) and identify two major populations: $CD206^+/CD301b^+$ and $CD206^+/CD301b^-$. The numbers of $CD206^+/CD301b^+$ macrophages increased concomitantly with repair, when the anti-inflammatory phenotype switch occurs in midstage healing. Using diphtheria toxin–mediated depletion models in mice, we show that selective depletion of midstage CD301b-expressing macrophages phenocopied wound healing defects observed in mice where multiple myeloid lineages are depleted. Additionally, when FACS-isolated subpopulations of myeloid cells were transplanted into 3-day wounds of syngeneic mice, only $CD206^+/CD301b^+$ macrophages significantly increased proliferation and fibroblast repopulation. These data show that the CD301b-expressing subpopulation of macrophages is critical for activation of reparative processes during the midstage of cutaneous repair.

INTRODUCTION

Restoration of skin after injury is essential for life and involves sequential regenerative phases involving immune, epithelial, and mesenchymal cells to reform the epidermis and its

Correspondence: Valerie Horsley, Department of Molecular, Cellular and Developmental Biology, Yale University, 219 Prospect Street, Box 208103, New Haven, Connecticut 06520, USA. valerie.horsley@yale.edu.

CONFLICT OF INTEREST
The authors state no conflict of interest.

SUPPLEMENTARY MATERIAL
Supplementary material is linked to the online version of the paper at www.jidonline.org, and at http://dx.doi.org/10.1016/j.jid.2016.05.107

Author Manuscript

underlying supportive dermis. Early stage repair is defined by inflammation, wherein myeloid cells, including neutrophils and then macrophages, are recruited to the injury site to clear pathogens and debris (Delavary et al., 2011; Eming et al., 2007). The midstage of healing consists of a proliferative phase in which macrophages promote robust migration and proliferation of keratinocytes to reseal the epidermal barrier and dermal regeneration via fibroblast and blood vessel restoration (Lucas et al., 2010; Mirza et al., 2010). During late stage wound healing, newly regenerated tissue is pruned and remodeled to resemble the cellular arrangement of nonwounded tissue (Brancato and Albina, 2011; Delavary et al., 2011).

The immune cell repertoire within skin wounds evolves with each repair stage and promotes distinct aspects of regeneration. After injury, $CD11b^+$/$F4\text{-}80^+$ macrophages are recruited to skin in a CCR2-dependent manner and express high levels of Ly6C ($Ly6C^{hi}$) (Ramachandran et al., 2012; Rodero et al., 2012; Willenborg et al., 2012) and inflammatory cytokines (Eming et al., 2007; Werner and Grose, 2003). Early stage macrophages are similar to classically activated or the M1 macrophages described by others (Brancato and Albina, 2011; Ferrante and Leibovich, 2012). Throughout healing, macrophage phenotype changes as macrophage cell surface protein and cytokine messenger RNA expression changes (Auffray et al., 2009; Brancato and Albina, 2011; Ferrante and Leibovich, 2012; Mirza and Koh, 2014). As regeneration proceeds into midstage healing, $CD11b^+$/$F4\text{-}80^+$/$Ly6C^{hi}$ macrophages decline, and the macrophage pool expresses mannose receptor (CD206), Fizz1, IL-10, transforming growth factor (TGF)-β1 and vascular endothelial growth factor (Daley et al., 2010; Mirza and Koh, 2014; Werner and Grose, 2003). These midstage macrophages, referred to as alternatively activated or M2 macrophages (Gordon, 2003; Martinez et al., 2008), mediate epithelial and dermal repair (Delavary et al., 2011; Knipper et al., 2015; Lucas et al., 2010). In the late phase of cutaneous repair, wound macrophages up-regulate metalloproteases to prune excess extracellular matrix to prevent scar formation (Duffield et al., 2005). The progression of macrophage phenotype after injury suggests that multiple populations of myeloid cells likely regulate specific aspects of regeneration.

Macrophages are essential for skin repair in adult mammals. Human chronic nonhealing venous leg ulcers or diabetic wounds in mice and humans display alterations in monocyte-derived cells (Goren et al., 2003; Mirza et al., 2013; Mirza and Koh, 2011; Wetzler et al., 2000). Furthermore, delayed healing in adult mice occurs when macrophages are depleted using anti-sera (Leibovich and Ross, 1975) or diphtheria toxin (DT)-induced death of monocyte-derived cells in genetic mouse models wherein DT receptor (DTR) is selectively expressed in these lineages (Goren et al., 2010; Lucas et al., 2010; Mirza et al., 2010). In the later experiments, DTR expression was induced by Cre recombinase activity under the *Lysozyme M* (*LysM*) promoter, which is expressed by monocytes, dendritic cells (DCs), and macrophages, or *CD11b*, which is expressed by macrophages and DCs (Auffray et al., 2009; Tamoutounour et al., 2013). Although these studies support the role of macrophages in skin repair, the precise cell type controlling skin regeneration within this heterogeneous and versatile lineage is not understood.

Author Manuscript Author Manuscript Author Manuscript Author Manuscript

Here, we investigated the contribution of specific macrophage subsets to reparative processes during skin regeneration by transplanting specific myeloid cells into skin wounds and depleting specific myeloid cells during wound healing in mice. Consistent with other groups (Knipper et al., 2015; Novak and Koh, 2013), we found that the macrophage phenotype switches from inflammatory to anti-inflammatory before re-epithelialization, fibroblast repopulation, and revascularization of skin wounds and that depleting midstage myeloid cells severely impairs multiple processes of cutaneous repair. Interestingly, we find that CD301b marks a portion of midphase macrophages and that depletion of CD301b-expressing macrophages is sufficient to phenocopy skin repair defects observed by depletion of myeloid cells more broadly. Transplanting CD301b^{+} macrophages is sufficient to enhance re-epithelialization, dermal proliferation, and fibroblast repopulation during midstage repair. Additionally, we showed that CD301b-expressing macrophage gene expression is enriched for growth factors and cytokines involved in skin regeneration. Therefore, our results identify a subset of CD301b^{+} macrophages critical for activating cutaneous repair during midstage wound healing.

RESULTS

Altered macrophage phenotype precedes skin regeneration

Because macrophage phenotype varies in different mouse backgrounds and wound paradigms, we sought to define the timing of myeloid cell plasticity compared with cutaneous regeneration after full-thickness excision of murine dorsal skin. We have previously shown in our wound paradigm that the early stage of healing in mice (1.5 days) corresponds to the inflammatory phase of injury (Daley et al., 2010; Eming et al., 2007), and that 3–5 days postinjury is the midstage or proliferative phase of repair when re-epithelialization, fibroblast repopulation, and revascularization occurs (McGee et al., 2012; Schmidt and Horsley, 2013) (see Supplementary Figure S1a and b online). Analysis of immune subsets showed that the number of viable macrophages (Sytox^{-}/CD45^{+}/CD11b^{+}/F4-80^{+}) increased 5 and 7 days after wounding compared with 1.5- and 3-day wounds (Figure 1a–c).

To assess broad macrophage classes in early versus midstage repair, we examined macrophage Ly6C and CD206 levels throughout healing using flow cytometry (Figure 1d). Although 1.5-day wounds were enriched for Ly6C^{hi} macrophages, most 3-day wound macrophages were CD206^{+} (Figure 1e). The percentage of CD206^{+} macrophages remained high 5 and 7 days after injury, similar to nonwounded skin, and these macrophages were enriched for cytokines and growth factors that promote repair (Figure 1f). These data are consistent with previous studies (Daley et al., 2010; Yin et al., 2013) and indicate that a wound bed macrophage phenotype switch precedes regeneration during the midstage of epidermal and dermal repair.

Midstage myeloid cells are required for cutaneous repair

To further examine the relationship between macrophage phenotype and cutaneous repair, we used a previously characterized mouse model that allows depletion of *LysM*-expressing myeloid cells (neutrophils, monocytes, and macrophages) through inducible expression of

Author Manuscript

Author Manuscript

Author Manuscript

Author Manuscript

the simian diphtheria toxin receptor (iDTR) upon expression of Cre recombinase driven by the *LysM* promoter (*LysMcre*/iDTR mice) (Buch et al., 2005; Clausen et al., 1999; Goren et al., 2010). After DT administration to mice at day 0 and 1 day after injury, we observed reduced CD11b$^+$/F4-80$^+$ wound macrophage numbers 3 days after injury in *LysMcre*/iDTR compared with control mice (Figure 2a and b).

Similar to previous studies (Goren et al., 2010; Lucas et al., 2010), continual depletion of LysM$^+$ myeloid cells resulted in healing impairment at 7 days, as indicated by abrogation of re-epithelialization, proliferation, and fibroblast and blood vessel regeneration (Figure 2c–h and see Supplementary Figure S2a–c online). To explore whether myeloid cells function distinctly in early versus middle stage skin regeneration, we depleted LysM$^+$ cells during the early and midstage healing process. Because myeloid cell numbers recover within 2 days of DT treatment, we targeted early stage myeloid cells with DT administration at day –0.5 and day 0.5 after injury. Midstage myeloid cells were targeted by DT administration 3, 4, and 6 days postinjury (Figure 2c). When LysM$^+$ myeloid cells were depleted during early stage wound healing, the ensuing 7-day wound beds appeared histologically similar to control wounds because re-epithelialization, proliferation, and revascularization were similar to control wound beds; however, we observed a reduction in ER-TR7$^+$ fibroblast regeneration (Figure 2c–h and see Supplementary Figure S2a–c). This slight difference in early wound bed phenotype compared with that reported in previous studies (Lucas et al., 2010) may reflect differences in wounding and DT administration paradigms. In contrast, depleting LysM$^+$ myeloid cells during the midstage of healing resulted in poorly healed wounds with defects in re-epithelialization, proliferation, fibroblast regeneration, and revascularization (Figure 2c–h and see Supplementary Figure S2a–c). Overall, these data confirm previous work that midstage myeloid cells are required for multiple reparative processes (Goren et al., 2010; Lucas et al., 2010; Mirza et al., 2010).

Midstage myeloid cells enhance dermal repair

To determine if a low number of myeloid cells from midstage wounds can enhance cutaneous repair, we transplanted 30,000 LysM$^+$ myeloid cells into 3-day wounds and analyzed regeneration 5 days after injury. LysM$^+$ myeloid cells were isolated from *LysM*cre;mT/mG mice in which *LysM*cre mediated a heritable switch from membrane-bound td-Tomato to membrane-bound green fluorescent protein (GFP) expression (mT/mG) (Muzumdar et al., 2007) (see Supplementary Figure S3a online). Because we observed skin repair peaking 5 days after injury (see Supplementary Figure S1a and b), we isolated GFP$^+$ (myeloid cells) and Tomato$^+$ (nonmyeloid cells) cells from 5-day wound beds (see Supplementary Figure S3a); injected them into 3-day wound beds of mT/mG-negative, syngeneic littermates; and harvested tissue 5 days after injury. To examine proliferation during repair, 5-ethynyl-2′-deoxyuridine (EdU) was administered to mice on days 3 and 4 postinjury (see Supplementary Figure S3a). Transplanted cells persisted 2 days after injection (see Supplementary Figure S3b). Wounds from mice injected with myeloid cells did not show enhanced re-epithelialization but contained a greater percentage of EdU-incorporating cells, increased numbers of phosphorylated histone (pH3)$^+$ cells/mm^2, increased ER-TR7$^+$ fibroblast repopulation, and blood vessel formation in wounds transplanted with myeloid cells compared with nonmyeloid cells (see Supplementary Figure

Author Manuscript Author Manuscript Author Manuscript Author Manuscript

S3c–g), showing that midstage myeloid cells promoted wound bed proliferation, fibroblast repopulation, and revascularization. Collectively, these data indicate that midstage myeloid cells are capable of promoting reparative processes in dermal repair.

Macrophage heterogeneity during the midstage of wound healing

*LysM*cre displays Cre activity in several myeloid cell types (Clausen et al., 1999; Goren et al., 2010) and thus does not define a specific macrophage subtype. We hypothesized that a specific macrophage subclass functions to support regeneration during midstage repair. To examine macrophage heterogeneity during wound healing, we analyzed the expression of CD206, which is expressed by midstage macrophages in skin wounds (Daley et al., 2010; Mirza and Koh, 2011), and CD301b, also expressed by M2 macrophages (Raes et al., 2004) (Figure 3a). Although most $CD11b^+$/$F4\text{-}80^+$ macrophages express both $CD206^+$ and $CD301b^+$ in uninjured skin, relatively few macrophages have cell surface expression of both proteins in 1.5-day wounds. At this early stage of repair, approximately 40% of $CD206^+$ macrophages present in wound beds express CD301b (Figure 3b). During midstage healing, the percentage of $CD11b^+$/$F4\text{-}80^+$ macrophages expressing CD206 and CD301b increases (Figure 3a and b); 3 days postinjury, 50% of $CD11b^+$/$F4\text{-}80^+$/$CD206^+$ macrophages express CD301b, and this percentage increases to approximately 80% 5 days after injury (Figure 3a and b and see Supplementary Figure S4a and b online). These data indicate that macrophages are heterogeneous in vivo during wound healing and show that CD301b expression increases as macrophage phenotype changes during midphase skin regeneration.

$CD301b^+$ macrophages are necessary for skin repair

To examine the contribution of $CD301b^+$ cells to skin regeneration, we depleted $CD301b^+$ cells during repair using mice expressing a DTR/GFP fusion protein under the endogenous CD301b promoter (macrophage galactose-type C-type lectin 2 or *Mgl2*)(*Mgl2*$^{DTR/GFP}$). This mouse model has been used to successfully deplete dermal CD301b-expressing cells with high efficiency (Kumamoto et al., 2013). We observed a complete ablation of GFP^+ cells in wound beds 1 day after DT injection to *Mgl2*$^{DTR/GFP}$ mice (see Supplementary Figure S4c and d), with a reduced number of $CD301b^+$ cells 2 days after injection (Figure 3c). $CD206^+$ macrophages were still abundant in wounds of DT-treated *Mgl2*^{DTR} mice (see Supplementary Figure S4e).

To determine if $CD301b^+$ macrophages contribute to midstage skin regeneration, we depleted $CD301b^+$ cells 3 days after injury in *Mgl2*$^{DTR/GFP}$ mice and examined wound beds after 5 and 7 days (Figure 3c). Immunostaining of skin sections with antibodies against ER-TR7 and α-smooth muscle actin showed defects in fibroblast/myofibroblast repopulation in 5- and 7-day wound beds of DT-treated *Mgl2*$^{DTR/GFP}$ mice (Figure 3d and e). We also detected decreases in re-epithelialization, EdU incorporation, and revascularization in DT-treated *Mgl2*$^{DTR/GFP}$ mice (Figure 3d and e and see Supplementary Figure S4f). These healing defects phenocopy *LysM*cre mice treated with DT during midstage healing (Figure 2c–h) and indicate that $CD301b^+$ cells are a specific subset of cells that contribute to skin regeneration.

Author Manuscript Author Manuscript Author Manuscript Author Manuscript

CD301b^{+} macrophages enhance skin regeneration

Since transplanting myeloid cells from 5-day wounds into 3-day recipient wound beds increased fibroblast and vascular regeneration (see Supplementary Figure S3), we determined if a low number of CD301b^{+} macrophages could stimulate a similar effect. We used FACS to isolate cellular subsets from 5-day wounds for cell transplantation into 3-day wound beds and examined the contribution of four cell populations to repair in syngeneic littermate control animals: nonimmune stromal cells (CD45^{-}) as a control, monocytes (CD45^{+}/CD11b^{+}/F4-80^{-}), CD206^{+}/CD301b^{-} macrophages, and CD206^{+}/CD301b^{+} macrophages. EdU was administered on days 3 and 4 after injury, and wounds were examined at day 5 (Figure 4a). Strikingly, we detected an increase in re-epithelialization, EdU^{+} incorporating cells, mitotic pH3^{+} cells/mm^{2}, and relative fluorescence of ER-TR7^{+} fibroblasts in wounds injected with CD206^{+}/CD301b^{+} macrophages compared with vehicle control and CD206^{+}/CD301b^{-} macrophages (Figure 4b and c); however, we did not detect a statistically significant change in revascularization.

To determine if CD301b^{+}/CD206^{+} macrophages express cytokines that facilitate epidermal and/or dermal repair, we examined messenger RNA levels in CD206^{+} and CD301b^{+} macrophages. We find that CD206^{+}/CD301b^{+} macrophages express increased levels of *IL10*, *Pdgfβ*, and *Tgfβ1* compared with the stromal vascular fraction and did not express *Fgf7* or *Tgfβ3*, which are growth factors produced by wound bed fibroblasts (Figure 4d). Taken together, these results implicate CD301b-expressing macrophages as a key cell type responsible for activating reparative processes during skin wound healing.

DISCUSSION

Our data show that a specific class of myeloid cells, CD301b^{+} macrophages, is essential for midstage healing of skin after injury. This conclusion is based on major defects in cutaneous repair (re-epithelialization, angiogenesis, and fibroblast regeneration) when CD301b-expressing macrophages are depleted during midstage repair. This dysfunctional regeneration phenocopies defects observed when the myeloid lineage is ablated more broadly during midphase skin regeneration using *LysM*cre and *CD11b*cre (Goren et al., 2010; Lucas et al., 2010; Mirza et al., 2010). In addition, we also show that transplantation of CD11b^{+}/F4-80^{+}/CD301b^{+} cells, but not CD301b^{-} cells, promotes proliferation of cells in the wound bed and fibroblast recruitment to skin wounds during midphase repair. We only observed increased re-epithelialization after injection of CD301b^{+} macrophages and not total myeloid cells, showing the enriched regenerative potential of this macrophage subset. Because the proportion of CD301b^{+} cells increased during midstage healing, our data show that CD301b^{+} macrophages coordinate midstage skin regeneration after injury.

Although CD301b is expressed by a subset of dermal DCs (CD11b^{+} cells), where it participates in the uptake of *N*-acetylgalactosamine residues (Kawakami et al., 1994), and DT treatment of *Mgl2*$^{DTR/GFP}$ mice has been shown to deplete CD11b^{+} DCs and Langerhans cells (Kumamoto et al., 2013), we hypothesize that CD301b^{+} macrophages are the primary myeloid cell type involved in coordinating midstage regeneration in skin after injury. Because we did not observe significant numbers of CD11b^{+}/F4-80^{-}/MHCII^{+}/CD301b^{+} DCs in skin wound beds during the early or midstages of repair (not shown), we

Author Manuscript

Author Manuscript

Author Manuscript

Author Manuscript

hypothesize the more prevalent CD11b$^+$/F4-80$^+$/CD206$^+$/CD301b$^+$ macrophage population is the key cell type involved in midstage wound repair. Consistent with this hypothesis, transplantation of CD11b$^+$/F4-80$^+$/CD301b$^+$ cells is sufficient to enhance re-epithelialization, dermal proliferation, and fibroblast recruitment similar to transplantation of total myeloid cells, suggesting that these are essential cells that coordinate midstage skin repair. Finally, our data show that CD301b$^+$ macrophages express several cytokines including IL-10, platelet-derived growth factor–β and TGF-β1 that mediate regeneration during skin wound healing (Brancato and Albina, 2011; Knipper et al., 2015; Werner and Grose, 2003). Future studies exploring whether specific DC subsets or Langerhans cells function in cutaneous repair and additional studies examining additional heterogeneity within CD301b$^+$ macrophages during skin healing will be of great interest.

The nature of the myeloid cell plasticity during tissue repair is not clear (Gordon and Taylor, 2005; Novak and Koh, 2013). Our data and those of others (Daley et al., 2010; Lucas et al., 2010; Willenborg et al., 2012) show that myeloid cells display distinct phenotypes during repair, yet how these phenotypes are generated is poorly understood. It is possible that CD301b$^+$ cells are formed from myeloid cells resident in skin or derived from circulating myeloid cells in a CCR2-dependent manner. Because CD206$^+$ macrophages are abundant in skin wounds of DT-treated *Mgl2*$^{DTR/GFP}$ mice, CD301b expression may indicate a maturation of CD206$^+$ cells during skin regeneration. Because *Mgl2* (CD301b) expression is downstream of signal transducer and activator of transcription-6 activation in response to IL-4 or IL-13 stimulation (Raes et al., 2004), it is possible that CD206$^+$/CD301b$^+$ macrophages represent recently described macrophages that control collagen fibril assembly during skin regeneration (Knipper et al., 2015); however, because anti-inflammatory macrophages exist in *IL-4* receptor knock-out mice (Daley et al., 2010; Ferrante et al., 2013), *Mgl2* activation could be independent of IL-4 receptor signaling or other regenerative macrophage populations could exist during skin wound healing. Future studies using lineage tracing of myeloid cells during skin injury may show lineage relationships between subsets of myeloid cells.

In summary, our data identify a specific “pro-healing” myeloid cell population that functions during cutaneous repair. Further study of CD301b$^+$ macrophages may reveal molecular mechanisms by which myeloid cells function in tissue repair. Furthermore, induction of obesity and/or diabetes (Seitz et al., 2010) in *Mgl2*$^{DTR/GFP}$ mice will allow the investigation of how this myeloid subset contributes to diabetes-impaired skin repair, which displays defects in myeloid cells (Mirza and Koh, 2011, 2014; Mirza et al., 2013). Finally, because myeloid cells function in multiple tissues to control regeneration after injury, our identification of a role of CD301b$^+$ myeloid cells in skin repair may have broad implications for regeneration of many tissue types.

MATERIALS AND METHODS

Mice

All animal care and experiments followed guidelines issued by Yale University’s Institutional Animal Care and Use Committee. C57/Bl6 mice were purchased from Charles River, and previously described *LysM*cre (stock #004781), iDTR (stock #007900), and

Author Manuscript

Author Manuscript

Author Manuscript

Author Manuscript

mT/mG (stock #007676) were purchase from Jackson Laboratories (Bar Harbor, ME). *Mgl2*$^{DTR/GFP}$ mice were developed by the laboratory of A. Iwasaki (Yale University, New Haven, CT) (Kumamoto et al., 2013). For wounding studies, 7–9-week-old male mice were used during the telogen phase of hair cycling. Mice were anesthetized with isofluorane, and four or six full-thickness wounds, 3–4 mm apart, were made on shaved dorsal skin using a 4-mm biopsy punch (Accuderm, Ft. Lauderdale, FL). For EdU experiments, 50 mg/kg of EdU (Invitrogen, Waltham, MA) was injected intraperitoneally at indicated time points and detected per the manufacturer's protocol. To genetically deplete myeloid cells, *LysM*cre/iDTR mice were given 50 μl of 20 ng/μl DT (Sigma, St. Louis, MO) via tail vein injection. To deplete CD301b-expressing cells, 25 μl of 20 ng/μl DT was administered intraperitoneally to *Mgl2*$^{DTR/GFP}$ mice.

Immunofluorescence and morphometric analysis

Wound beds were mounted in optimum cutting temperature compound (Tissue-Tek, Sakura Finetek USA, Torrance, CA) and sectioned through their entirety to identify the center of the wound bed. Next, 14-μm cryosections were fixed with 4% formaldehyde and immunostained as previously described (Festa et al., 2011; McGee et al., 2012) using the following antibodies: CD31 (rat, 1:100; BD Biosciences, Franklin Lakes, NJ,), CD206 (rat, 1:500; Biolegend, San Diego, CA), CD301b (rat 1:200; eBioscience, San Diego, CA), ER-TR7 (rat, 1:500; Abcam, Cambridge, UK), GFP (chicken, 1:1,000; Abcam,), and phosphohistone H3 (rabbit, 1:500; Abcam). Histological quantification for each wound bed was conducted on the three central-most sections, and the averages from two wounds were averaged for each animal. Re-epithelialization and corrected total fluorescence were calculated using ImageJ software (National Institutes of Health, Bethesda, MD) as described previously (McGee et al., 2012; Schmidt and Horsley, 2013). Revascularization was calculated using Adobe Photoshop to measure the total CD31^{+} pixels divided by the total number of pixels in wound beds.

Fluorescence-activated cell sorting and analysis

Mouse back skin and wound beds were dissected and digested into single cells using 1:100 collagenase 1A (Worthington, Lakewood, NJ), as previously described (Festa et al., 2011; Schmidt and Horsley, 2013). Single-cell suspensions were resuspended in FACS staining buffer (1% BSA in phosphate buffered saline with 2 mmol/L EDTA) and stained with the following antibodies for 30 minutes on ice: CD45-APC-eFluor780 (1:2,000; eBioscience,), CD11b-Alexa700 (1:500; eBioscience), F4-80-eFluor450 (1:50; eBioscience), CD206-Alexa488 (1:500; Biolegend), CD301b-Alexa660 (1:100; eBioscience), Ly6C-APC (1:250; eBioscience). Wound macrophages were defined as CD45^{+}/CD11b^{+}/F4-80^{+} cells. Sytox Orange (1:100,000; Invitrogen) was added immediately before sorting with a FACS Aria III with FACS DiVA software (BD Biosciences). Flow cytometry analysis was performed using FlowJo Software (FlowJo, Ashland, OR).

Real-Time PCR

For quantitative real-time PCR, samples were FACS purified directly into TRIzol LS (Invitrogen), RNA was extracted, and complementary DNA was generated using Superscript III Reverse Transcriptase (Thermo Fisher, Waltham, MA) per the manufacturer's

Author Manuscript Author Manuscript Author Manuscript Author Manuscript

instructions. Primers (5′–3′, forward and reverse): *CD206*, CAAGGAAGGTTG GCATTTGT and CCTTTCAGTCCTTTGCAAGC; *CD301b*, GACTGAGTTCTCGCCTCTGG and CTGGGAAGGAATTAGAGCAAACT; *IL10*, GCCCAGAAATCAAGGAGCATT and TGCTCCACTGCCTTG CTCTTA; *Pdgfβ*, CCCTGTGTGGAGGTGCAGCG and GACACGGC CCAGGTCACACG; *Tgfβ1*, ACGCCTGAGTGGCTGTCTTTTGAC and GGGCTGATCCCGTTGATTTCCACG; *Tgfβ3*, CGTTTCAATGTGTCC TCAGTGGAG and AAGAGCTCAATTCTCTGCTCTGTG; *Fgf7*, AGC GGAGGGGAAATGTTCG and TCCAGCCTTTCTTGGTTACTGAGA; and *β-actin*, ATCAAGATCATTGCTCCTCCTGAG and CTGCTTG CTGATCCACATCTG. All quantitative real-time PCR was performed using SYBR green on a LightCycler 480 (Roche, Basel, Switzerland) and normalized to *β-actin* as previously described (Festa et al., 2011).

Cell transplants

For transplanting cells into wounds, cell populations were FACS purified, counted using a hemocytometer, and diluted in FACS staining buffer at a concentration of 3.0×10^6 cells/ml. 10 μl of cell suspension (30,000 cells) was slowly injected into wound beds of anesthetized mice using a 30-guage needle.

Statistics

To determine significance between two groups, comparisons were made using Student *t* test. Analyses across multiple groups were made using a one-way analysis of variance with Bonferroni's post hoc test using GraphPad Prism for Mac (GraphPad Software, La Jolla, CA) with significance set at $P < 0.05$.

Supplementary Material

Refer to Web version on PubMed Central for supplementary material.

Acknowledgments

We thank VH's lab members for technical assistance, critically reading the manuscript, and discussions. VH is funded by the National Institutes of Health (AR06029S) and Connecticut Department of Public Health (12SCBYALE01). BS is a New York Stem Cell Foundation—Druckenmiller Fellow. This research was supported by the New York Stem Cell Foundation.

Abbreviations

DC	dendritic cell
DT	diphtheria toxin
DTR	diphtheria toxin receptor
EdU	5-ethynyl-2′-deoxyuridine
GFP	green fluorescent protein
iDTR	simian diphtheria toxin receptor
TGF	transforming growth factor

Author Manuscript Author Manuscript Author Manuscript Author Manuscript

References

Auffray C, Sieweke MH, Geissmann F. Blood monocytes: development, heterogeneity, and relationship with dendritic cells. Annu Rev Immunol. 2009; 27:669–92. [PubMed: 19132917]

Brancato SK, Albina JE. Wound macrophages as key regulators of repair. Am J Pathol. 2011; 178:19–25. [PubMed: 21224038]

Buch T, Heppner FL, Tertilt C, Heinen TJAJ, Kremer M, Wunderlich FT, et al. A Cre-inducible diphtheria toxin receptor mediates cell lineage ablation after toxin administration. Nat Methods. 2005; 2:419–26. [PubMed: 15908920]

Clausen B, Burkhardt C, Reith W, Renkawitz R, Forster I. Conditional gene targeting in macrophages and granulocytes using LysMcre mice. Transgenic Res. 1999; 8:265–77. [PubMed: 10621974]

Daley JM, Brancato SK, Thomay AA, Reichner JS, Albina JE. The phenotype of murine wound macrophages. J Leukoc Biol. 2010; 87:59–67. [PubMed: 20052800]

Delavary BM, van der Veer WM, van Egmond M, Niessen FB, Beelen RHJ. Macrophages in skin injury and repair. Immunobiology. 2011; 216:753–62. [PubMed: 21281986]

Duffield JS, Forbes SJ, Constandinou CM, Clay S, Partolina M, Vuthoori S, et al. Selective depletion of macrophages reveals distinct, opposing roles during liver injury and repair. J Clin Invest. 2005; 115:56–65. [PubMed: 15630444]

Eming SA, Krieg T, Davidson JM. Inflammation in wound repair: molecular and cellular mechanisms. J Invest Dermatol. 2007; 127:514–25. [PubMed: 17299434]

Ferrante CJ, Leibovich SJ. Regulation of macrophage polarization and wound healing. Adv Wound Care. 2012; 1:10–6.

Ferrante CJ, Pinhal-Enfield G, Elson G, Cronstein BN, Hasko G, Outram S, et al. The adenosine-dependent angiogenic switch of macrophages to an M2-like phenotype is independent of interleukin-4 receptor alpha (IL-4Rα) signaling. Inflammation. 2013; 36:921–31. [PubMed: 23504259]

Festa E, Fretz J, Berry R, Schmidt B, Rodeheffer M, Horowitz M, et al. Adipocyte lineage cells contribute to the skin stem cell niche to drive hair cycling. Cell. 2011; 146:761–71. [PubMed: 21884937]

Gordon S. Alternative activation of macrophages. Nat Rev Immunol. 2003; 3:23–35. [PubMed: 12511873]

Gordon S, Taylor PR. Monocyte and macrophage heterogeneity. Nat Rev Immunol. 2005; 5:953–64. [PubMed: 16322748]

Goren I, Allmann N, Yogev N, Schürmann C, Linke A, Holdener M, et al. A transgenic mouse model of inducible macrophage depletion. Am J Pathol. 2010; 175:132–47.

Goren I, Kämpfer H, Podda M, Pfeilschifter J, Frank S. Leptin and wound inflammation in diabetic ob/ob mice: differential regulation of neutrophil and macrophage influx and a potential role for the scab as a sink for inflammatory cells and mediators. Diabetes. 2003; 52:2821–32. [PubMed: 14578302]

Kawakami K, Yamamoto K, Toyoshima S, Osawa T, Irimura T. Dual function of macrophage galactose/N-acetylgalactosamine-specific lectins: glycoprotein uptake and tumoricidal cellular recognition. Jpn J Cancer Res. 1994; 85:744–9. [PubMed: 8071116]

Knipper JA, Willenborg S, Brinckmann J, Bloch W, Maaß T, Wagener R, et al. Interleukin-4 receptor a signaling in myeloid cells controls collagen fibril assembly in skin repair. Immunity. 2015; 43:803–16. [PubMed: 26474656]

Kumamoto Y, Linehan M, Weinstein JS, Laidlaw BJ, Craft JE, Iwasaki A. CD301b^{+} dermal dendritic cells drive T helper 2 cell-mediated immunity. Immunity. 2013; 39:733–43. [PubMed: 24076051]

Leibovich SJ, Ross R. The role of the macrophage in wound repair. A study with hydrocortisone and antimacrophage serum. Am J Pathol. 1975; 78:71–100. [PubMed: 1109560]

Lucas T, Waisman A, Ranjan R, Roes J, Krieg T, Muller W, et al. Differential roles of macrophages in diverse phases of skin repair. J Immunol. 2010; 184:3964–77. [PubMed: 20176743]

Martinez FO, Sica A, Mantovani A, Locati M. Macrophage activation and polarization. Front Biosci. 2008; 13:453–61. [PubMed: 17981560]

Author Manuscript
Author Manuscript
Author Manuscript
Author Manuscript

McGee HM, Schmidt BA, Booth CJ, Yancopoulos GD, Valenzuela DM, Murphy AJ, et al. IL-22 promotes fibroblast-mediated wound repair in the skin. J Invest Dermatol. 2012; 133:1321–9. [PubMed: 23223145]

Mirza R, DiPietro LA, Koh TJ. Selective and specific macrophage ablation is detrimental to wound healing in mice. Am J Pathol. 2010; 175:2454–62.

Mirza RE, Fang MM, Ennis WJ, Koh TJ. Blocking interleukin-1β induces a healing-associated wound macrophage phenotype and improves healing in type 2 diabetes. Diabetes. 2013; 62:2579–87. [PubMed: 23493576]

Mirza R, Koh TJ. Dysregulation of monocyte/macrophage phenotype in wounds of diabetic mice. Cytokine. 2011; 56:256–64. [PubMed: 21803601]

Mirza RE, Koh TJ. Contributions of cell subsets to cytokine production during normal and impaired wound healing. Cytokine. 2014; 71:409–12. [PubMed: 25281359]

Muzumdar MD, Tasic B, Miyamichi K, Li L, Luo L. A global double-fluorescent Cre reporter mouse. Genesis. 2007; 45:593–605. [PubMed: 17868096]

Novak ML, Koh TJ. Macrophage phenotypes during tissue repair. J Leukoc Biol. 2013; 93:875–81. [PubMed: 23505314]

Raes G. Macrophage galactose-type C-type lectins as novel markers for alternatively activated macrophages elicited by parasitic infections and allergic airway inflammation. J Leukoc Biol. 2004; 77:321–7. [PubMed: 15591125]

Ramachandran P, Pellicoro A, Vernon MA, Boulter L, Aucott RL, Ali A, et al. Differential Ly-6C expression identifies the recruited macrophage phenotype, which orchestrates the regression of murine liver fibrosis. Proc Natl Acad Sci USA. 2012; 109:E3186–95. [PubMed: 23100531]

Rodero MP, Hodgson SS, Hollier B, Combadiere C, Khosrotehrani K. Reduced Il17a expression distinguishes a Ly6c. J Invest Dermatol. 2012; 133:783–92. [PubMed: 23235530]

Schmidt BA, Horsley V. Intradermal adipocytes mediate fibroblast recruitment during skin wound healing. Development. 2013; 140:1517–27. [PubMed: 23482487]

Seitz O, Schiirmann C, Hermes N, Müller E, Pfeilschifter J, Frank S, et al. Wound healing in mice with high-fat diet- or ob gene-induced diabetes-obesity syndromes: a comparative study. Exp Diabetes Res. 2010; 2010:476969. [PubMed: 21318183]

Tamoutounour S, Guilliams M, Sanchis FM, Liu H, Terhorst D, Malosse C, et al. Origins and functional specialization of macrophages and of conventional and monocyte-derived dendritic cells in mouse skin. Immunity. 2013; 39:925–38. [PubMed: 24184057]

Werner S, Grose R. Regulation of wound healing by growth factors and cytokines. Physiol Rev. 2003; 83:835–70. [PubMed: 12843410]

Wetzler C, Kämpfer H, Stallmeyer B, Pfeilschifter J, Frank S. Large and sustained induction of chemokines during impaired wound healing in the genetically diabetic mouse: prolonged persistence of neutrophils and macrophages during the late phase of repair. J Invest Dermatol. 2000; 115:245–53. [PubMed: 10951242]

Willenborg S, Lucas T, van Loo G, Knipper JA, Krieg T, Haase I, et al. CCR2 recruits an inflammatory macrophage subpopulation critical for angiogenesis in tissue repair. Blood. 2012; 120:613–25. [PubMed: 22577176]

Yin H, Li X, Hu S, Liu T, Yuan B, Gu H, et al. IL-33 accelerates cutaneous wound healing involved in upregulation of alternatively activated macrophages. Mol Immunol. 2013; 56:347–53. [PubMed: 23911389]

Author Manuscript
Author Manuscript
Author Manuscript
Author Manuscript

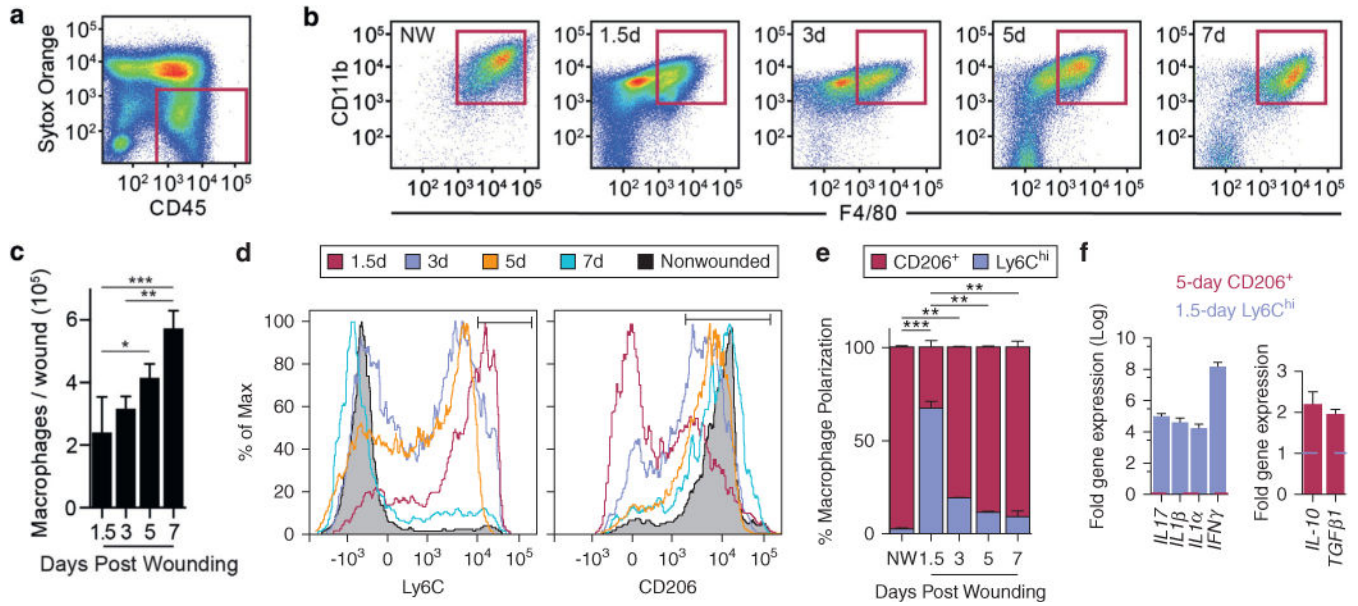

Figure 1. Macrophage phenotypic switch during cutaneous repair

(**a, b**) Representative FACS dot plots of (**a**) Sytox$^-$/CD45$^+$ gating for analysis of CD11b$^+$/F4-80$^+$ macrophages (red box) in nonwounded and indicated time points after injury. (**c**) Quantification of **b**. (**d**) Representative FACS histogram of Ly6C and CD206 on wound bed macrophages. (**e**) Quantification of the percentage of Ly6C^{hi} or CD206$^+$ CD11b$^+$/F4-80$^+$ macrophages within wound beds at indicated time points. (**f**) Fold change in messenger RNA for cytokines in 1.5-day Ly6C^{hi} wound macrophages (purple bar and line) versus 5-day CD206$^+$ wound macrophages (red bar and line) macrophages. $n = 3–4$ mice for each time point. All data are mean ± standard error of the mean. *$P < 0.05$; **$P < 0.01$; ***$P < 0.001$. d, day; NW, nonwounded.

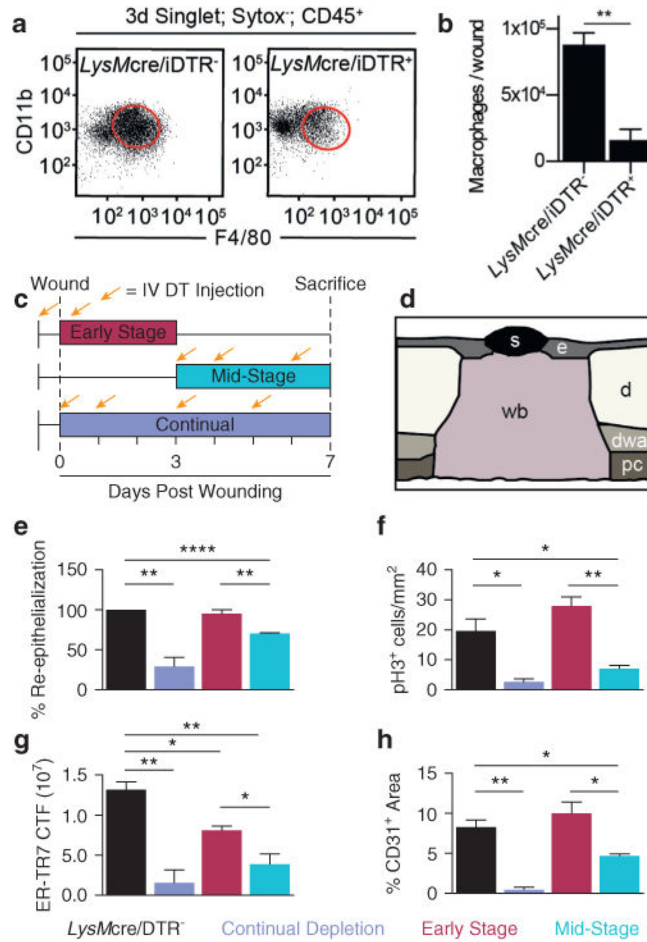

Figure 2. Midstage myeloid cells are necessary for wound healing

(**a**) FACS dot plots of CD11b$^+$/F4-80$^+$ cells in 3-day wound beds after diphtheria toxin administration immediately before and 1 day after injury. (**b**) Quantification of **a**. $n = 4$ mice for each time point. (**c**) Schematic illustrating experiments ablating myeloid cells continually and during the early (0–3 days after injury) and middle (3–7 days after injury) stages of skin repair. Orange arrows indicate diphtheria toxin injections. (**d**) Schematic illustration of an excisional wound bed. Quantification of (**e**) re-epithelialization, (**f**) phosphohistone H3$^+$ cells, (**g**) relative fluorescence of ER-TR7 immunoreactivity and (**h**) wound bed area of CD31$^+$ immunoreactivity in 7-day *LysM*cre/iDTR myeloid cell-depleted wound beds. $n = 4$ mice for each condition. All data are mean ± standard error of the mean. *$P < 0.05$, **$P < 0.01$, ***$P < 0.001$, ****$P < 0.0001$. d, dermis; DT, diphtheria toxin; dwat, dermal white adipose tissue; e, epidermis; iDTR, simian diphtheria toxin receptor; IV, intravenous; pc, panniculus carnosis; s, scab; wb, wound bed.

Author Manuscript Author Manuscript Author Manuscript Author Manuscript

Author Manuscript

Author Manuscript

Author Manuscript

Author Manuscript

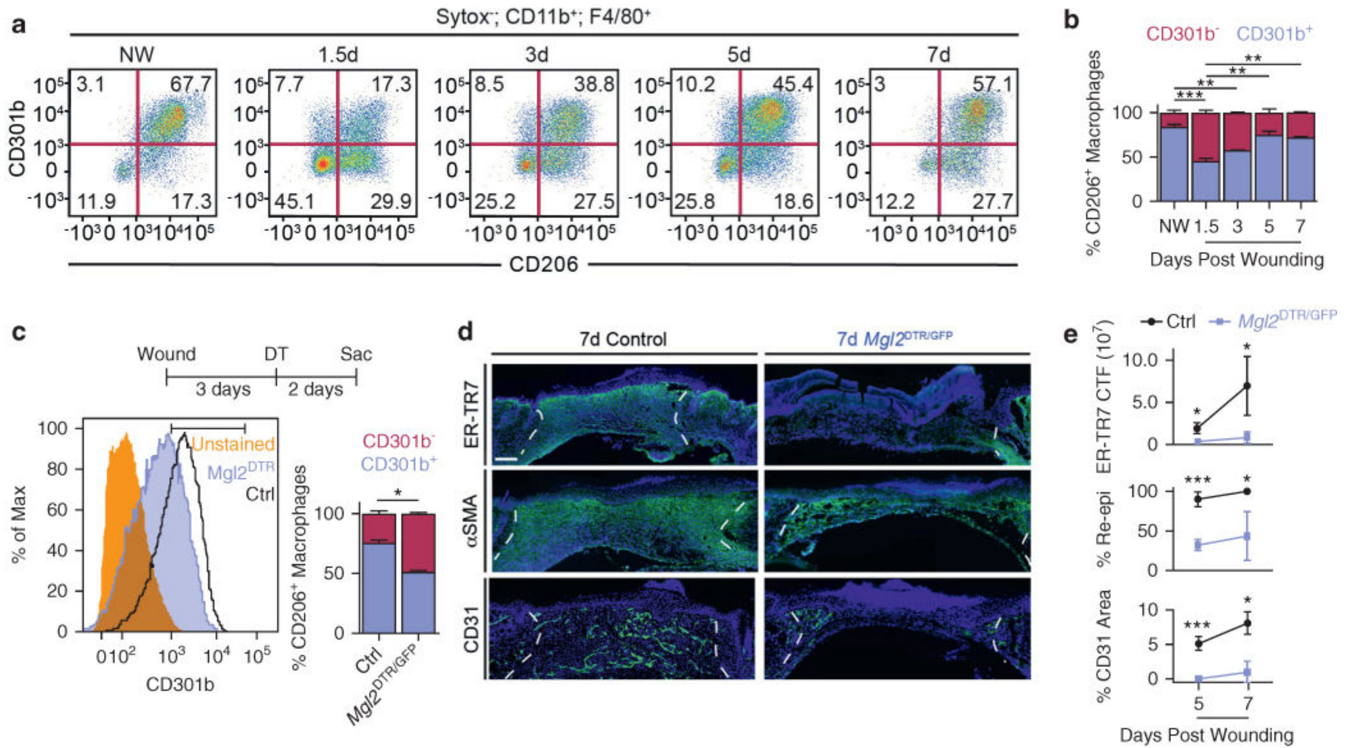

Figure 3. CD301b-expressing macrophages are required for skin repair

(**a**) Representative FACS dot plots of Sytox$^-$/CD11b$^+$/F4-80$^+$ cells for CD301b and CD206 throughout healing. (**b**) Quantification of the percentage of CD301b$^-$ (red) or CD301b$^+$ (purple) (CD11b$^+$/F4-80$^+$/CD206$^+$) macrophages. $n = 3$ mice for each bar. (**c**) Representative FACS histogram and quantification of CD301b$^+$ cells in 5-day wounds in diphtheria toxin-treated Mgl2$^{DTR/GFP}$and control mice. $n = 3$ mice for each condition. (**d**) Images of 7-day wounds immunostained for ER-TR7, α-smooth muscle actin, and CD31. (**e**) Quantification of ER-TR7 corrected total fluorescence, re-epithelialization (re-epi), and wound bed area containing CD31 fluorescence in diphtheria toxin-treated *Mgl2*$^{DTR/GFP}$ and control wounds. $n = 5$ mice for each condition. Scale bar = 250 μm. White lines delineate wound edges. All data are mean ± standard error of the mean. *$P < 0.05$, **$P < 0.01$, ***$P < 0.001$. Ctrl, control; d, day; DT, diphtheria toxin; Max, maximum; NW, nonwounded; re-epi, re-epithelialization; Sac, sacrifice.

Author Manuscript

Author Manuscript

Author Manuscript

Author Manuscript

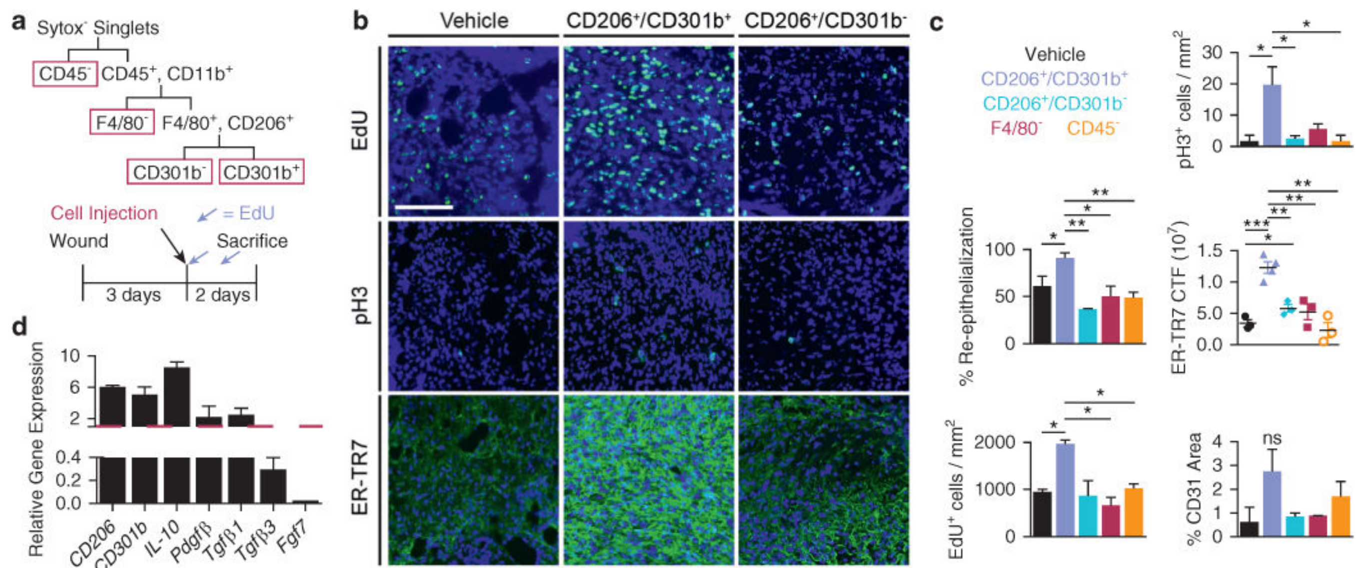

Figure 4. CD301b-expressing macrophages enhance dermal repair

(**a**) Hierarchical gating strategy used to FACS sort 5-day wound bed cells for transplantation into 3-day syngeneic littermates. (**b**) Representative images of EdU^+, $pH3^+$, and $ER\text{-}TR7^+$ cells in the middle of 5-day wound beds of mice that were transplanted with vehicle, $CD206^+/CD301b^+$, or $CD206^+/CD301b^-$ macrophages. (**c**) Quantification of re-epithelialization, EdU^+, and $pH3^+$ cells per mm^2, ER-TR7 corrected total fluorescence, and wound bed area containing CD31 fluorescence in 5-day wound beds transplanted with indicated cell types. (**d**) Real-time PCR analysis of messenger RNA in $CD206^+/CD301b^+$ macrophages 5 days after wounding. Red line indicates gene expression in total wound bed. $n = 3$ mice for each bar. Scale bar = 200 μm. All data are mean ± standard error of the mean. $*P < 0.05$, $**P < 0.01$, $***P < 0.001$. ns, not significant.